Loosely Coupled GPS/INS Integration with Kalman filtering for land vehicle applications

Le Nhat Hieu, Vinh Hao Nguyen

Abstract— **Nowadays, global positioning system (GPS) has been used widely in land vehicles to provide positioning services. However, information from this stand-alone device may be interrupted under some circumstances such as: urban environment, under the tunnels, etc. In addition, low-rate sample time typically 1Hz is another drawback of GPS. Therefore, GPS receiver can be augmented with the inertial navigation system (INS) to provide faster positioning information. By fusing GPS and INS data, the errors are bounded and accuracy increases considerably even when using low-cost INS and GPS. This paper presents a method of INS/GPS integration where a loosely coupled model is formulated and an extended Kalman filter is then applied to estimate information about position, velocity, and acceleration. Experiment results show that the processing time is reduced significantly but the estimated errors are acceptable (less than 1 meters) when applying the proposed integration method under the good signal of GPS. The performance evaluation is also implemented on several road trajectories in urban city that the 3 meters precision could be reached. In addition, accurate positioning and navigation results are still available from 9 to 14 seconds of GPS outages with the position errors spread from 3 to 10 meters (RMS).**

I. Introduction

RECENTLY, land vehicle navigation system has drawn much attention in both researches and applications. Nowadays, GPS is the popular solution for most of navigation systems. However, several error sources (multipath, atmospheric effects, clock error, etc) can deteriorate the quality of the position and velocity from GPS signal besides its low rate update. On the other hand, Inertial Measurement Units (IMUs) can provide high rate of up-to-date data (acceleration and rotation rate of the object) that can be used in many automobile dead-reckoning and aviation applications as well. Although, MEMs technology can reduce the IMU's cost considerably, it could make IMU's results diverge after continuously using for a long period of time. By integrating GPS and INS, this hybridization solution provides remarkable results than each of those stand-alone systems.

GPS-aided INS has found its applications both in military and civilian such as: UAV, cruise missile, navigation system in cars and ships, etc with different ranges of accuracy and prices. A common IMU which was used in military applications costs more than $200.000 with the position error less than 30 m/hr. Meanwhile, the position error of an IMU in automotive application, which costs less than $10.000, is much higher (more than 30km/min). Therefore, many researchers have tried to enhance the performance of the low-cost GPS/INS system, for instance Eun-Hwan Shin (2001), Adriano Solimeno (2007)

In [3], the author discussed the integration of a Honeywell HG1700 IMU with one DGPS antenna. Eun-Hwan Shin aims to improve the accuracy of low-cost IMU so that they can be used as a stand-alone navigation system during GPS outages. Besides, he also proposed and tested several techniques such as: field calibration methods, velocity matching alignment, using the non-holonomic constraints.

In [2], the author paid his attention to the combination of a Crista IMU from Cloud Cap Technology with one GPS antenna. Both loosely coupled and tightly coupled schemes were surveyed during his thesis to compare the performance in different experiments.

On the other hand, the author in [1] used 3 MEMs gyros (ADXRS-150) and 3 accelerometers (ADXL-201) separately. His goal is to achieve the good navigation results in urban city with low-cost devices by proposing some methods called numerical considerations for the covariance matrix P, filter tuning and lever-arm correction. Moreover the influences of different error sources on the results are also discussed.

The purpose of this paper is to combine the [2] and [3] with some modifications. There is only one Kalman filter in the loosely-coupled integration scheme instead of two filters by using the Garmin commercial GPS. The state-space vectors in the fusion filter decrease from 27-elements to 15-elements. Furthermore, non-holonomic velocity constraints are applied to improve the performance for the land vehicle navigation system. Many experiments have also been conducted to find out how long INS can follow trajectories while GPS outages occur. More importantly, these results can also be achieved with the low –cost sensors as well. In this experiment, it costs 800$ for the whole package

This paper is organized in the following manners. Section II will briefly investigate the navigation system and derives necessary parameter for the fusion. The integration GPS/INS will be discussed in Section III. Section IV presents implementation results, and conclusions in Section V.

L. N. Hieu is with Faculty of Electrical & Electronics Engineering, HoChiMinh City University of Technology, Vietnam. (e-mail: nhathieu_gc2005@yahoo.com).
V. H. Nguyen is with Faculty of Electrical & Electronics Engineering, HoChiMinh City University of Technology, Vietnam. (e-mail: vinhhao@hcmut.edu.vn).

II. NAVIGATION ALGORITHM

Integration of GPS and INS using loosely-coupled scheme is shown in Fig.1. In this application, both systems are independent of each other. The INS block, which is shown here, consists of Inertial Measurement Unit (IMU) and INS kinematic equations.

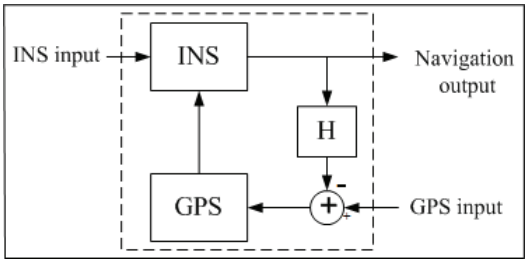

Figure 1. Loosely Coupled with Feedback [1]

A. Kinematic INS equations:

The major of dead reckoning navigation composes of two main parts: propagation of attitude reference and solutions of navigation equations. The former uses gyroscope outputs to calculate the attitude of the body coordinate frame with respect to the reference coordinate frame. The latter uses this parameter to compose a transformation matrix which converts coordinate vectors (acceleration outputs, gravity force, velocity, etc) to obtain the acceleration of the body coordinate.

The coordinate in which computations is performed, is usually chosen between one of the two: ECEF frame (e-frame) or Local geodetic frame (n-frame). Here we chose n-frame with the position, velocity are expressed as follows:

$$r^n = \begin{bmatrix} \varphi & \lambda & h \end{bmatrix}^T \tag{1}$$

$$v^n = \begin{bmatrix} V_N & V_E & V_D \end{bmatrix}^T \tag{2}$$

From [3], the continuous-time nonlinear dynamical equations in n-frame are:

$$\begin{bmatrix} \dot{r}^n \\ \dot{v}^n \\ \dot{R}_b^n \end{bmatrix} = \begin{bmatrix} D^{-1}v^n \\ R_b^n f^b - \left(2w_{ie}^n + w_{en}^n\right) \times v^n + g^n \\ R_b^n \left(\Omega_{ib}^b - \Omega_{in}^b\right) \end{bmatrix} \tag{3}$$

Where R_b^n is transformation matrix from body frame to n-frame, Ω_{ib}^b is skew-symmetric matrix of angular velocity vector w_{ib}^b of the b-frame respect to the i-frame (inertial frame) coordinated in the b-frame, the Ω_{in}^b skew-symmetric matrix of angular velocity vector w_{in}^b of the n-frame respect to the i-frame (inertial frame) coordinated in the b-frame and finally f^b is the special force vector outputted by the accelerometer in body frame.

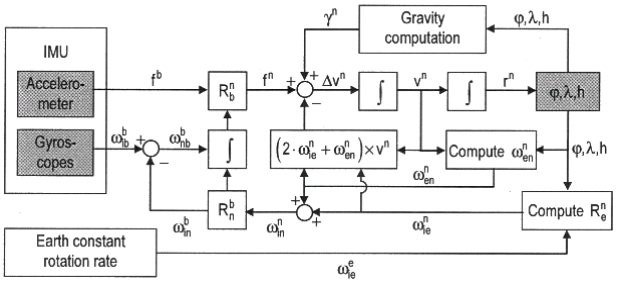

Figure 2. INS mechanization in n-frame [2].

The state-space vectors of Kalman filter consists of the INS error dynamic equations and INS error model. We will discuss how to get these parameters in the following parts.

B. INS errors dynamic equations:

The errors dynamic equations can be obtained by perturbing the kinematic equations. The linearized position, velocity, attitude error dynamics, which can be written as [3], are expressed as follows:

$$\Delta\dot{r}^n = F_{rr}\delta r^n + F_{rv}\delta v^n \tag{4}$$

$$\Delta\dot{v}^n = F_{vr}\delta r^n + F_{vv}\delta v^n + \left(f^n \times\right)\varepsilon^n + R_b^n f^b \tag{5}$$

$$\Delta\dot{\varepsilon}^n = F_{er}\delta r^n + F_{ev}\delta v^n + \left(w_{in}^n \times\right)\varepsilon^n + R_b^n \delta w_{ib}^b \tag{6}$$

Where ε^n is the attitude errors and δf^b presents perturbations of the special force in b-frame while $\delta\omega_{ib}^b$ denoting the perturbation of the angular rate of b-frame with respect to i-frame coordinated in b-frame.

C. INS error model:

The experiment is conducted on ADIS16354 IMU with factory calibrated sensitivity, bias and alignment. Therefore, Scale factors and Turn-on bias drift of IMU can be omitted. This paper only takes the bias drift of accelerometer and gyroscope into account. These two biases can be modeled with several types of processes. In this work, a first-order Gauss-Markov process has been used [2]:

$$\delta\dot{b}_x(t) = \frac{1}{T_{b,x}}\delta b_x(t) + w_{b,x}(t) \tag{7}$$

where:

$T_{b,x}$: Time-constant of Gauss-Markov process.

$w_{b,x}$: White Gaussian noise with zero mean and the power spectral density is q.

III. DATA FUTION OF KALMAN FILTERING USING NON-HOLONOMIC VELOCITY CONSTRAINTS.

The state vector of the Kalman filter consists of following 15 elements which are the INS error dynamic equations together with the INS error models:

$$x = \begin{bmatrix} \delta r^n & \delta v^n & \varepsilon^n & \delta b_a & \delta b_g \end{bmatrix}^T \tag{8}$$

A. *Kalman filter model:*

The continuous system model for the Kalman filter is characterized by the followings vector and matrices:

$$\dot{x}(t) = F(t)x(t) + G(t)w(t) \tag{9}$$

Where F is the dynamic matrix, G is the design matrix and is the forcing vector function:

$$F = \begin{bmatrix} F_{rr} & F_{rv} & 0_{3\times3} & 0_{3\times3} & 0_{3\times3} \\ F_{vr} & F_{vv} & \left(f^n\times\right) & R_b^n & 0_{3\times3} \\ F_{er} & F_{ev} & -\left(w_{in}^n\times\right) & 0_{3\times3} & R_b^n \\ 0_{3\times3} & 0_{3\times3} & 0_{3\times3} & -diag\left(1/T_{b,a}\right) & 0_{3\times3} \\ 0_{3\times3} & 0_{3\times3} & 0_{3\times3} & 0_{3\times3} & -diag\left(1/T_{b,g}\right) \end{bmatrix} \tag{10}$$

$$G = \begin{bmatrix} 0_{3\times3} & 0_{3\times3} \\ R_b^n & 0_{3\times3} \\ 0_{3\times3} & -R_b^n \\ 0_{3\times3} & 0_{3\times3} \\ 0_{3\times3} & 0_{3\times3} \end{bmatrix} \tag{11}$$

$$w = \begin{bmatrix} w_a & w_g \end{bmatrix}^T \tag{12}$$

The element ω is the white nose with the covariance matrix as follows:

$$E\left[w(t)w(\tau)^T\right] = Q(t)\delta(t-\tau) \tag{13}$$

Where the symbol δ denotes the Dirac delta function and $Q(t)$ is the power spectral density of the white noise $w(t)$

$$Q = \begin{bmatrix} diag(q_a) & 0_{3\times3} \\ 0_{3\times3} & diag(q_g) \\ 0_{3\times3} & 0_{3\times3} \\ 0_{3\times3} & 0_{3\times3} \\ 0_{3\times3} & 0_{3\times3} \end{bmatrix} \tag{14}$$

Where q_a and q_g are the power spectral density of 3D accelerometer and gyroscope.

Because our system is implemented with high-speed sample data rate, we need to transform our model into discrete form [4].

$$x_{k+1} = \phi_k x_k + w_k \tag{15}$$

Where ϕ_k is the state transition matrix and:

$$\phi_k \approx I + F\Delta t \tag{16}$$

$$E\left[w_k {w_i}^T\right] = \begin{cases} Q_k, & i = k \\ 0, & i \neq k \end{cases} \tag{17}$$

The covariance matrix associated to the discrete-time noise vector can be determined by the following approximated expression [3]

$$Q_k \approx \frac{1}{2}\left[\phi_k G(t_k)Q(t_k)G^T(t_k) + G(t_k)Q(t_k)G^T(t_k){\phi_k}^T\right]\Delta t \tag{18}$$

The observation equations used to update the Kalman filter are the differences between GPS and INS computed position and velocity vector. However, in order to avoid the numerical instabilities when calculating the Kalman gain we need to multiple the first two rows by $(R_M + h)$ and $(R_N + h)\cos\varphi$ respectively:

$$z_k = H_k x_k + v_k \tag{19}$$

Which define the measurement vector at one epoch of time as the combination of state-space vector and measurement error. Where:

$$z = \begin{bmatrix} (R_M + h)\left(\varphi_{INS} - \varphi_{GPS}\right) \\ (R_M + h)\cos\varphi\left(\lambda_{INS} - \lambda_{GPS}\right) \\ h_{INS} - h_{GPS} \\ v_{INS}^n - v_{GPS}^n \end{bmatrix} \tag{20}$$

$$H = \begin{bmatrix} R_M + h & 0 & 0 & 0_{1\times3} & 0_{1\times9} \\ 0 & (R_M + h)\cos\varphi & 0 & 0_{1\times3} & 0_{1\times9} \\ 0 & 0 & 1 & 0_{1\times3} & 0_{1\times9} \\ 0_{3\times1} & 0_{3\times1} & 0_{3\times1} & I_{3\times3} & 0_{3\times9} \end{bmatrix} \tag{21}$$

The covariance of the measurement noise and its relationship with the system noise are expressed as follows:

$$E\left[v_k v_i^T\right] = \begin{cases} R_k, & i = k \\ 0, & i \neq k \end{cases} \tag{22}$$

$$E\left[w_k w_i^T\right] = 0 \quad \forall i,k \tag{23}$$

$$R = \begin{bmatrix} \sigma_\varphi^2 & 0 & 0 & 0 & 0 & 0 \\ 0 & \sigma_\lambda^2 & 0 & 0 & 0 & 0 \\ 0 & 0 & \sigma_h^2 & 0 & 0 & 0 \\ 0 & 0 & 0 & \sigma_{V_N}^2 & 0 & 0 \\ 0 & 0 & 0 & 0 & \sigma_{V_E}^2 & 0 \\ 0 & 0 & 0 & 0 & 0 & \sigma_{V_D}^2 \end{bmatrix} \tag{24}$$

B. *Non-holonomic velocity constraints:*

The land vehicle velocity constraints are obtained due to the facts that the vehicle tends to travel in constant direction and does not jump off the ground. So the velocity on the perpendicular plane to the main directions can be assumed almost zero.

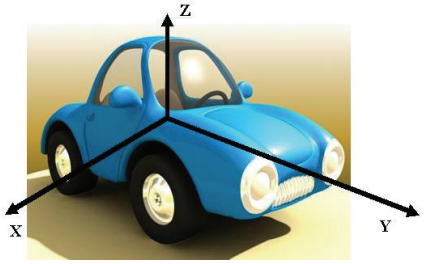

Figure 3. Car model travels primarily on the Y-direction [6].

This idea is used as a complementary Kalman filter which extracts the velocity of INS solutions as a measurement

observation to keep the position and velocity errors bounded. The implementation of non-holonomic velocity constraints are shown in the Fig.4:

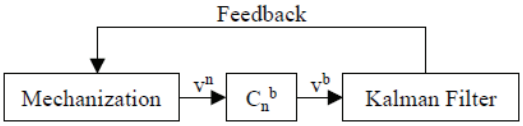

Figure 4. Implementation of velocity constraints [3].

By assuming that direction of vehicle forward velocity vector follows the X- axis of IMU. So:

$$v_y^b = \eta_y \tag{25}$$

$$v_z^b = \eta_z \tag{26}$$

Where η_i is the measurement noise value due to the presence of the slide slip caused by engine and the surface of the tested trajectory. The strength of the noise can be chosen to reflect the expected constraints violations.

The discretization of the measurement equations can be expressed as [4], where C_{ij} is the (i,j)-th element of DCM matrix R_b^n:

$$z_k = H_k x_k + v_k \tag{27}$$

$$z_k = \begin{bmatrix} v_y^b & v_z^b \end{bmatrix}^T \tag{28}$$

$$Hk = \begin{bmatrix} 0_{1\times3} & C_{12} & C_{22} & C_{32} & 0_{1\times6} & -v_D C_{22} + v_E C_{32} \\ 0_{1\times3} & C_{13} & C_{23} & C_{33} & 0_{1\times6} & -v_D C_{23} + v_E C_{33} \\ \cdots & v_D C_{12} - v_N C_{32} & & -v_E C_{12} + v_N C_{22} & & \cdots \\ & v_D C_{13} - v_N C_{33} & & -v_E C_{13} + v_N C_{23} & & \end{bmatrix} \tag{29}$$

$$E\left[v_k v_i^T \right] = \begin{cases} R_k, & i = k \\ 0, & i \neq k \end{cases} \tag{30}$$

IV. IMPLEMENTATION.

A. Experimental set-up:

In this study, the experimental data collection was carried out using a small test vessel that included a battery on the bottom and the inertial sensor, commercial GPS and the central DSP chip on the top. Besides there is also one separated laptop to control and acquire data.

The IMU used for this research were the high precision tri-axis inertial sensor ADIS16354 with the factory calibrated sensitivity, bias and alignment. The low-cost commercial GPS 18X LVC of Garmin with the embedded receiver and an antenna were chosen. The total cost for these two sensors take about 800$ (700$ for IMU and 100$ for GPS). Raw IMU measurements were recorder at 100Hz while GPS data were logged at 1Hz. Both GPS and INS data were sampled by TMS 320F28335 chip and then this DSP chip transmits the integrated data to laptop for processing. The whole system is shown in Figure 5.

B. Trajectory:

The map illustrating where the experiment was conducted is shown in Fig 6 this area is located far away from downtown with the clear-space environment with no high building surrounded. So the accuracy of GPS can reach to 3 meters. The test vessel was installed on the vehicle which was driven about 4.38km with 15 km/h average speed in 12.5 minutes.

a) Platform for GPS/INS data collection

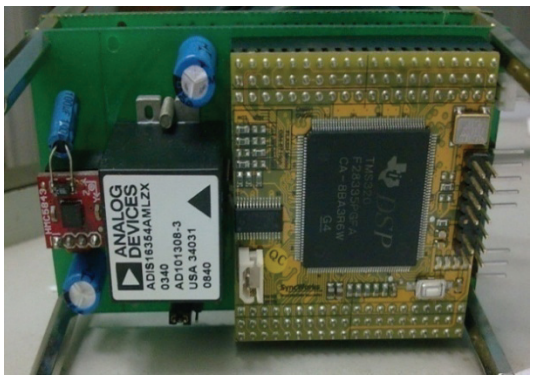

b) 9-DOF IMU board with angular rate, acceleration, magnetic measurement

Figure 5. Test vessel with IMU board on the top

Figure 6. Trajectory in Google Earth.

C. Test results:

Because of the absence of appropriate verifying

equipment, there is no reference trajectory log. Consequently, it is not possible to draw any firm conclusions regarding the position errors. However, with the clear-space environment when the experiment is conducted we can probably use the GPS results to consider the result from INS aided GPS system.

Figure 7 shows 12.5 minutes estimated trajectory in both e-frame and n-frame of the vehicle with an average velocity and frequent turns. Notice that, the vehicle was ridden in the close-loop routine consecutively for 3 times.

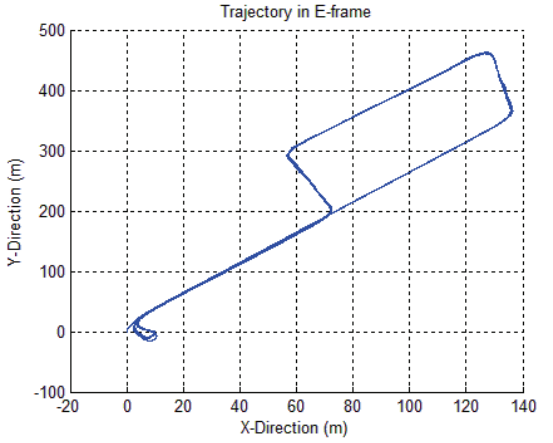

Figure 7. INS/GPS trajectory in both E-frame and n-frame

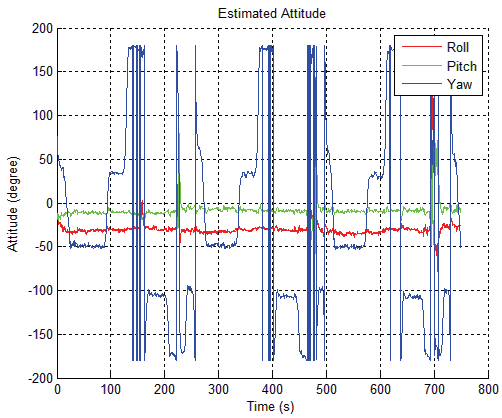

Figure 8. Estimated attitude of GPS/INS system

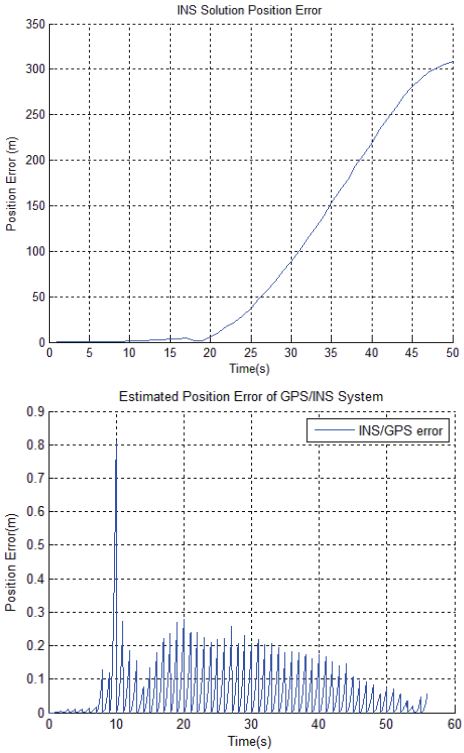

Fig.9. Position errors in GPS/INS system versus INS solution only

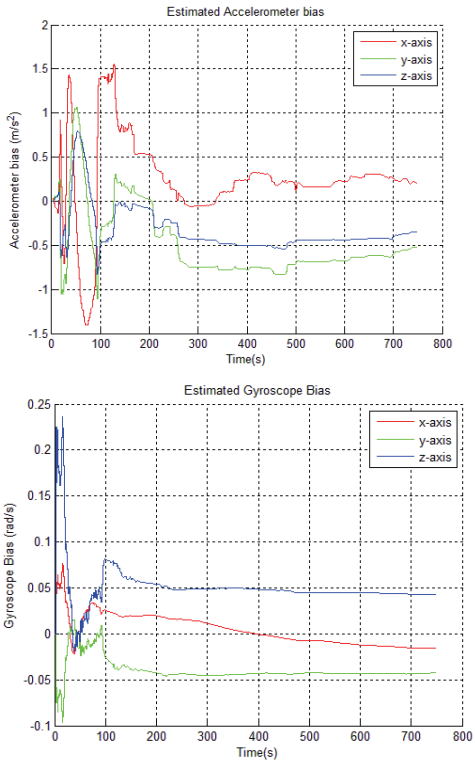

Figure 10. Estimated accelerometers and gyroscopes bias.

The estimated attitude of GPS/INS system is shown as in Fig.8. Because the vehicle merely travels in the x-y plane so only estimated roll angle changes dramatically in period due to the repetition of the trajectory. Noticing that sometimes the pitch and yaw angles reach extremely high, the possible explanation is that there is a vibration in the engine at this time.

Fig.9 show that without the precise INS error model the position errors could reach 300m after 50s. And when aiding GPS, our estimated position errors can achieve up to 0,5 meter.

The Kalman filter will easily diverge if the covariances are not chosen from the specific range. This action will also determine how long the estimated bias of accelerometers and gyroscopes will converge. Fig.10 shows these biases respect to time. The accelerometers take about 100s to converge while gyroscopes seem to converge after 100s.

Figure 11 shows the stimulated trajectory when GPS outages occur in 14 seconds and in 9 seconds. Because there is no measurement update for the filter, the trajectory is the result of INS solution and non-holonomic velocity constraints. However the estimated positions still drift remarkably more than 10m in 14s and 3m in 9s. But the high confidence GPS position brings back the trajectory when the next measurement is available. The Table 1 has been drawn after investigating the trajectory tendency during a long term of GPS outages.

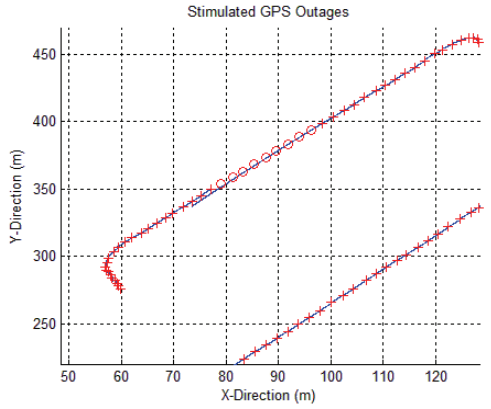

a) GPS outtages in 14s

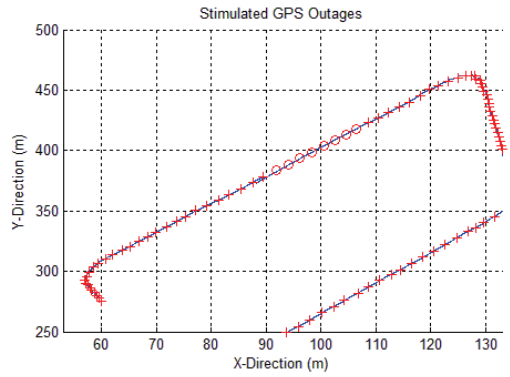

b) GPS outtages in 9s

Figure11. Trajectory while GPS outages occur

TABLE I
ESTIMATED POSITION ERROR DURING GPS OUTAGES

GPS OUTAGES (SECOND)	ESTIMATED ERROR (METER)	TRAJECTORY
3s	1m	Follow
5s	1.8m	Follow
9s	3m	Begin to drift
14s	10m	Diverge

V. CONCLUSION

This paper has shown an effective combination of two separated systems (GPS and INS) which have their own advantages and drawbacks. The low-cost IMU is a self-obtained sensor which is not capable of determining reasonable position information. GPS, in contrast, gives good results, but is only able to calculate every single second. In general, this paper has shown the basic integration method of GPS and INS and estimation techniques. Different results and conclusion has been also drawn upon this paper.

ACKNOWLEDGMENT

This research is funded by National Science & Technology Foundation of Vietnam (No. KC03.TN16/11-15) and Vietnam National University HoChiMinh City (VNU-HCM) under grant number B2012-20-09.

REFERENCES

[1] A.Schumacher, "Integration of a GPS aided Strapdown Inertial Navigation System for Land Vehicles," M.S thesis, Dept. Electro. Eng, Royal Institute of Technology, Stockholm, Sweden, 2006.

[2] A.Solimeno, "Low-Cost INS/GPS Data Fusion with extended Kalman Filter for Airborne Applications," M.S thesis, Aerospace.Eng, Universidade Tecnica de lisboa, 2007.

[3] E.H.Shin, "Estimation Techniques for Low-cost Inertial Navigation,", Phd thesis, Dept. of Geomatics Engineers, Calgary, Alberta, CA, 2005.

[4] G.Dissanayake, S.Sukkarieh, E.Nebot and H.D.Whyte, "The Ading of a Low-cost Strapdown Inertial Measurement Unit Using Vehicle Model Constraints for Land Vehicle Application," *IEEE Trans.Robotics and Automation,* Vol.17, pp.731-747, No.5, October,2001.

[5] G.Dissanayake, S.Sukkarieh, E.Nebot and H.D.Whyte, "The Ading of a Low-cost Strapdown Inertial Measurement Unit Using Vehicle Model Constraints for Land Vehicle Application," *IEEE Trans.Robotics and Automation,* Vol.17, pp.731-747, No.5, October,2001.

[6] T.D.Tan, L.M.Ha, N.T.Long, N.D.Duc, N.P.Thuy, "Land-vehicle mems INS/GPS positioning during GPS signal blockage periods," *VNU journal of Science, Mathematics – Physics 23*, pp.243-251, 2007.